DOI: 10.2478/v10077-009-0007-z

A. Krella
The Szewalski Institute of Fluid-Flow Machinery, Polish Academy of Sciences, Cavitation Group, ul. Fiszera 14, 80-231 Gdansk, Poland

CAVITATION RESISTANCE OF TiN NANOCRYSTALLINE COATINGS WITH VARIOUS THICKNESS

ABSTRACT

TiN nanocrystalline coatings of various thicknesses deposited on austenitic stainless steel, X6CrNiTi18-10, by means of the cathodic arc evaporation method were investigated in a cavitation tunnel with a slot cavitator. The estimated cavitation resistance parameters of the coatings were the incubation period and total mass loss. It was found that the incubation periods of the 4 μm and 7.8 μm-thick TiN coatings were over two and half times longer than that of the uncoated X6CrNiTi 18-10 steel and the total mass losses of these coatings were approximately half lower than of the uncoated specimen. The scanning electron microscope analysis indicated that the damage process of the TiN-4 coating originates from the micro-folding and coating fracture arises on the top of the micro-folds, whiles the TiN-8 and TiN-12 coatings were removed in the form of thin flakes. The factors mainly responsible for cavitation resistance of the TiN coatings are ability to plastic deformation of the coating and coating adhesion.

Key words: *nanocrystalline TiN coatings, degradation, fracture, impact*

INTRODUCTION

Nowadays the most machining tools, such as drills, hobs, mills, and cutting inserts are normally coated with titanium nitride (TiN) to prolong their lifetime and to improve the working efficiency. Ti-based coatings were the first developed ceramic coating systems and the most popular coatings for commercial applications. TiN thin films are used for high wear applications where they are regularly subject to cyclic loading during machining. Their main benefits are based on the combination of high hardness and toughness, properties which are especially important in conditions of dynamic impact wear when high cyclic local loading is the main cause of coating degradation, e.g. in impact wear of machine parts. Cavitation test can be a tool for studies of deformation, crack initiation and propagation in thin hard coatings.

Cavitation damage caused by repeating action of imploding cavitation bubbles in the vicinity of solid surface is a source of failure of pumps, valves, sharp bends. The collapse of the cavitation bubbles implies that an impulse is applied, typically by an impacting micro-jet or by a pressure wave impact. Because of high velocity of the impacting jet with several 100 m/s [1,2], short pulse duration approximately 2-3 μs or less [1], pressure pulses in range from several kPa to several GPa [1, 2] and the radius of the pressure wave in range from 80 μm to 2 mm [3], the degradation mechanism has

mainly mechanical, impact character. The implosions of cavitation bubbles cause uneven stress fields in the material and strengthening of the surface layer [4, 5]. The depth of strengthening depends on cavitation intensity, exposure time, the depth of deformity penetration and the yield stress of the material [4, 5] Inhomogeneity of deformities leads to cracking just below the strengthened layer and extraction of material particles from surface layer [4-7]. The course of cavitation erosion depends on the material itself, the intensity of the phenomenon and the kind of fluid. Because fracture initiation and its progress are dependent on the load history the materials degradation is considered to have fatigue character. Material investigations [4-7] proved that cavitation resistance of conventional materials depend on mechanical parameters (hardness, Young's modulus, tensile strength, fatigue strength), microstructure (grain sizes, phases, number of material defects) and also on surface roughness.

Owing to stain-hardening caused by repeated collapse of the cavities, the damage of the material has an entirely different aspect from typical fatigue damage, for which the name "cavitation fatigue" is often used. This suggests that materials, to be cavitation resistant, should possess high fatigue resistance. It was also noticed that good mechanical property correlation for many materials is between hardness and fatigue resistance. As the hardness and fatigue resistance are important to thin surface layer, the surface treatment techniques are thought to be effective.

As it was mention above, the increase of cavitation resistance was affected by the reduction of grain size for many materials with approximately similar mechanical properties. Nanomaterials, which possess mentioned above property: high hardness, high fatigue resistance and very small grains, are supposed to have good cavitation resistance. Nanocrystalline Ti-based coatings are the very common hard coatings used. Their impact wear [8-11], deformation behaviour [12] and cavitation resistance [13-16] have been investigated. Cavitation erosion investigations proved beneficial influence of nanocrystalline TiN coatings showing the importance of surface layer in initiating micro-cracks and their development. Although all defects in the coatings acted as nucleation centres for wear [13], all coated specimens revealed improved cavitation erosion resistance compared to uncoated steel [13-16].

The elastic strain to failure, which is regarded as the ratio of hardness and elastic modulus and is identified as the key characteristic for wear resistance [8, 17], was also found as the main coating factor in cavitation resistance [16]. Leyland and Matthews [17] emphasized the significance of a low value of elastic modulus for the improvement of wear resistance of ceramic coatings. Carried out investigations of TiN and Ti-Al-N coatings Yoon et al. [9] concluded that the so-called "plasticity index" H^3/E^{*2}, where H is hardness, $E^*=E/(1-v^2)$ E - Young's modulus, v – Poisson's coefficient, plays an important role in impact-wear behaviour of coating/substrate systems. They noticed that the impact-wear behaviour changed from plastic deformation to a brittle mode with the increase the "plasticity index". Similar results were obtained in Ref. [16]. Lima et al. [18] also noted the increased cavitation resistance of WC-Co coatings with a decreasing value of H/E ratio. They also found that cavitation erosion resistance increases proportionally with the coating fracture toughness K_C.

Disadvantage of the most coatings deposited on conventional materials is the problem with good adhesion assurance. The cavitation erosion tests of chromium nitride coatings showed that coatings with weak adhesion have partly spalled-off [19]. Investigation performed by Krella and Czyżniewski [16] confirmed that coatings with weak adhesion have partly spalled-off. Moreover, they achieved correlation adhesion with incubation period; an increase of critical load L_{C2} increased incubation period. The

critical load L_{C2} is the load, at which the coating removal from inside of the scratch starts. The incubation period is believed to be the most important stage due to change in dislocation structure and initiation micro-cracks.

The purpose of this work is to evaluate the effect of coating thickness on cavitation resistance of TiN coatings deposited on X6CrNiTi 18-10 austenitic stainless steel.

EXPERIMENTAL TECHNIQUES

The experimental tests were performed in a cavitation tunnel with a system of barricades. The schematic of the cavitation chamber is shown in Fig.1. Cavitation intensity is controlled by varying the slot width and the boost pump speed. Flow conditions are defined by the p_1 and p_2 absolute pressures measured at the chamber inlet and outlet respectively. Slightly hard tap water (5.9 mVal/dm^3) is used as the working liquid, temperature 20 $\pm$ 2^{o}C. The cavities (cavitating vortices and bubbles) are generated by the pressure decrease in the slot between two semi-cylindrical barricades.

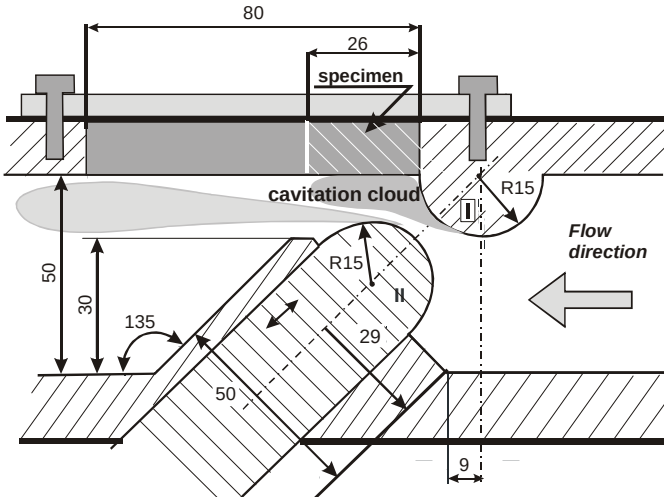

Fig. 1. Schematic view of cavitation chamber: I – stationary barricade, II – moving counter-barricade; the width of slot can be adjusted within the 0-15 mm range (all dimensions in mm)

Table 1. *Chemical compositions of the X6CrNiTi18-10 steel, wt. pct*

	C	Mn	Cr	Ni	Ti	Si	P	S
X6CrNiTi18-10	0.014	1.79	17.36	9.56	0.23	0.53	0.025	0.027

Table 2. *Properties of X6CrNiTi18-10 stainless steel*

Hardness [GPa]	Young's modulus [GPa]	Ultimate tensile strength [GPa]	Roughness (R_a) [μm]
1.7	199	0.684	0.02

The substrates (45mm x 26mm x 14 mm) of the X6CrNiTi18-10 austenitic steel were subjected to quenching at 1050^0C. Substrates were ground and polished to the roughness of $R_a \leq 0.05$ μm. The chemical composition of the X6CrNiTi18-10 steel is presented in Table 1 and basic properties in Table 2. The nanocrystalline TiN coatings were deposited by cathodic arc evaporation method (ARC) [16]. The typical process of coating deposition consists of pumping down to a vacuum below 2×10^{-3} Pa, heating the substrates to the temperature of 350^0C, cleaning the substrates by argon and titanium ions, initially deposition thin titanium interlayer (~ 0.1μm thickness) in the argon atmosphere and finally deposition of TiN coating in a nitrogen atmosphere occurred up to the thickness of approximately 4 μm, 8 μm and 12 μm. Parameters applied to the deposition of TiN coating are presented in Table 3.

Table 3. *Deposition parameters of TiN coatings [16]*

Pressure of residual gases	2×10^{-3} Pa
Working pressure of argon	1 Pa
Working pressure of nitrogen	1 Pa
Arc current	85 A
Substrate bias voltage	- 100 V
Substrate temperature	350^oC

The phase compositions of coatings were tested on a DRON2 X-ray diffractometer using CuKα radiation. The grain size was determined by means of the Scherrer method with reflex parameters (location and FWHM) using Gaussian analysis. The coating morphology was examined with JEOL JSM 5500 LV scanning electron microscope (SEM). The hardness and Young modulus were measured with a NanoHardness Tester (CSEM) using the method of Oliver and Pharr [20]. A scratch tester Revetest® produced by CSEM was used to investigate the coating adhesion. Basic properties of the TiN coatings deposited on X6CrNiTi18-10 steel are shown in Table 4. The H/E coefficient is the ratio of hardness (H) and elastic modulus (E). The critical load L_{C1} is defined by occurrence of the first cohesive failure of the coating, that is the cracks caused by tensile stresses inside and on the edges of the scratch behind the sliding diamond cone. The critical load L_{C2} is the load at which the coating removal from inside of the scratch starts

Table 4. *Properties of TiN coatings*

		TiN-4	TiN-8	TiN-12
Hardness, H [GPa]		21.7	26.1	30.7
Young's modulus, E [GPa]		344	433	525
H/E coefficient		0.063	0.060	0.058
Coating thickness [μm]		3.9	7.8	11.9
Adhesion	L_{C1} [N]	10	12	10
	L_{C2} [N]	23	33	34
Roughness (R_a) [μm]		0.35	0.36	0.38

The TiN coatings comprised of the stoichiometric regular phase of δ-TiN. The X-ray diffraction spectra (Fig. 2) show strong intensity of TiN (111). The diffraction intensities of TiN (200) and TiN (220) were found to gradually increase with coating thickness. According to the Scherrer method of (111) reflexes, the size of TiN crystallites has been estimated to be approximately 16 nm. With the increase of coating thickness the coating hardness increased. The hardness was found to be in the range of 21.7– 30.7 GPa. The elastic modulus was within the range of 344 – 525 GPa (Table 4).

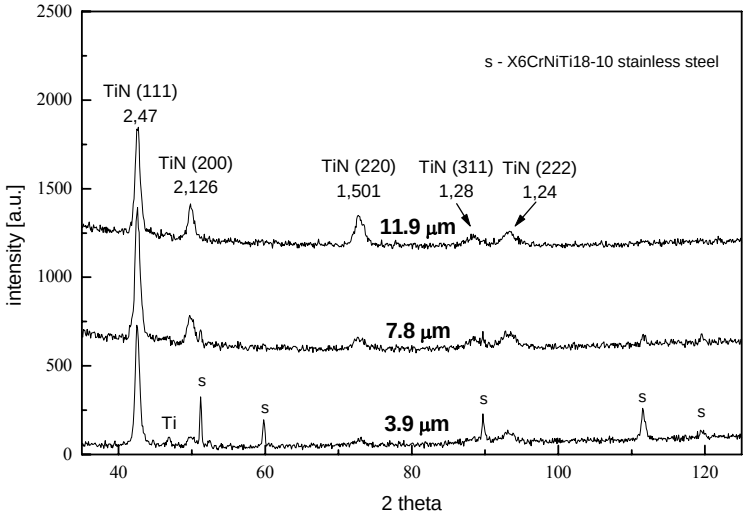

Fig. 2. X-ray diffraction patterns of the TiN coatings

The fracture images and morphology of the TiN coatings are shown on Fig. 3. All coatings are characterized by a compact fine crystalline microstructure (Fig. 3). Impurities visible on the coatings surface are Ti(N) microdroplets. These microdroplets always occur when the cathodic arc evaporation method is used. It is worth noting that with the increase of coating thickness the number of Ti(N) microdroplets increased. Moreover, Ti(N) microdroplets caused discontinuity in coating structure in the form of cavities inside the coatings with thickness of 7.8 and 11.9 μm (Fig. 3).

The results for the adhesion testing of TiN coatings are presented in Table 4. Taking into account the low hardness of the X6CrNiTi18-10 steel (about 2 GPa) and its large plastic deformation under substantial pressure of the Rockwell indenter, used for the scratch test, the examinations show good adhesion of the TiN coatings to this type of substrate. The first minor cracks occurred with a scratch made under the load of 10 N for TiN-4 and TiN-12 coatings and 12 N for TiN-8 coating. It corresponds to the critical load L_{C1} defined by occurrence of the first cohesive failure of the coating, that is the cracks caused by tensile stresses inside and on the edges of the scratch behind the sliding diamond cone. The critical loads L_{C2} at which coating removal from inside of the scratch starts and coating's adhesion attests were 23 N, 33 N and 34 N for TiN-4, TiN-8 and TiN-12 (Table 4), respectively. It was found that coating adhesion increases with rising coating thickness. The highest increase in adhesion L_{C2} took place in the increase of coating thickness from 3.9 μm to 7.8 μm.

The TiN coated specimens were subjected to cavitation impingement in the cavitation chamber operated with inlet pressure p_1 = 1000 kPa, outlet pressure p_2 = 130 kPa and a slot width of 5 mm. The coated specimens were marked TiN-4, TiN-8, TiN-12 where the number after the dash represents the coating thickness. In order to obtain

the erosion curves, the mass loss measurement was performed after each exposure interval. Before the test and after each test interval the specimens were cleaned, dried and reweighed. At the beginning of the cavitation test the measurements were conducted every 30 min of exposure (for the first 180 min of test) to estimate the incubation period. The duration of exposure intervals was then gradually increased. The total cavitation test duration was 600 min. After cavitation test the cavitation erosion damage was analysed with the scanning electron microscope (SEM).

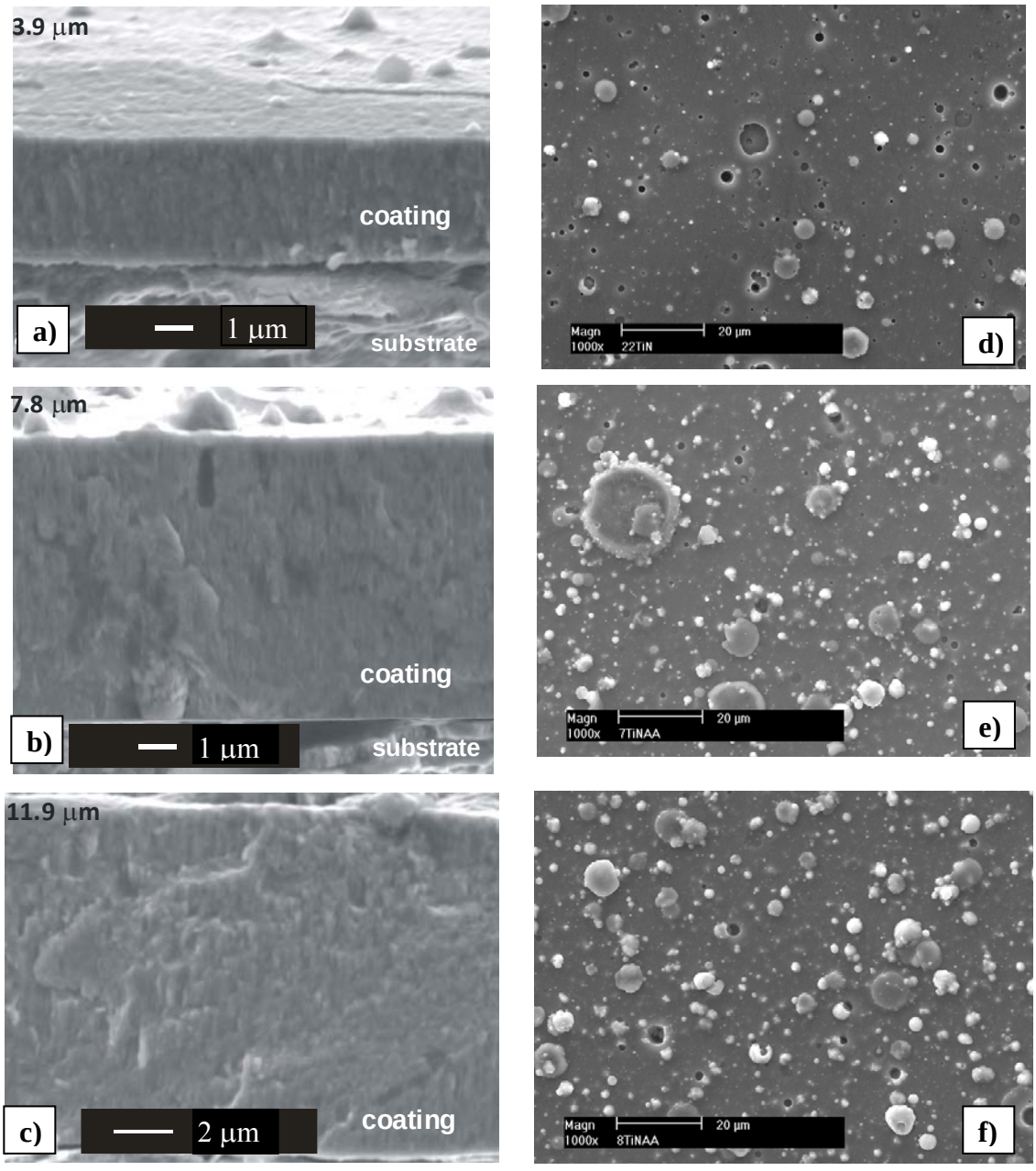

Fig. 3. SEM fracture images of TiN-4 (a), TiN-8 (b) and TiN-12 (c) coatings and SEM surface images of TiN-4 (d), TiN-8 (e) and TiN-12 (f) coatings

RESULTS

The cavitation curves of the TiN coatings deposited on X6CrNiTi18-10 stainless steel and of the uncoated X6CrNiTi18-10 steel during cavitation tests are shown in Fig. 5. The incubation period of an uncoated stainless steel was less than 90 min whereas for TiN-4, TiN-8 was less than 240 min. The incubation period of TiN-12 specimen lasted less than 30 min. The incubation period of TiN-4 and TiN-8 was over two times longer than the incubation period of uncoated X6CrNiTi18-10 steel. In case of TiN-12 a mass loss started at the beginning of cavitation test. This was likely correlated with the highest number of microdropples Ti(N) on TiN-12.

At incipient erosion Ti(N) microdroplets were removed from the coating surface; after that no mass loss took place for about 1 hour of exposure. This was noticed on nearly each coated specimen. The break in mass loss is connected with phase transformation $\gamma \rightarrow \alpha$ of the austenitic stainless steel, which always occurs despite the deposition of the TiN coating [15]. Afterward solid particles of hard coating or/and steel substrate / coating system were torn away. The highest mass loss of 6 mg occurred at TiN-12 specimen. The mass losses after the whole tests were 4 mg for both TiN-4, TiN-8; the mass loss of uncoated X6CrNiTi18-10 steel was 7 mg. It is worth noticed that cavitation curves of TiN-4 and TiN-8 are similar. All coated specimens had less mass loss than uncoated stainless steel.

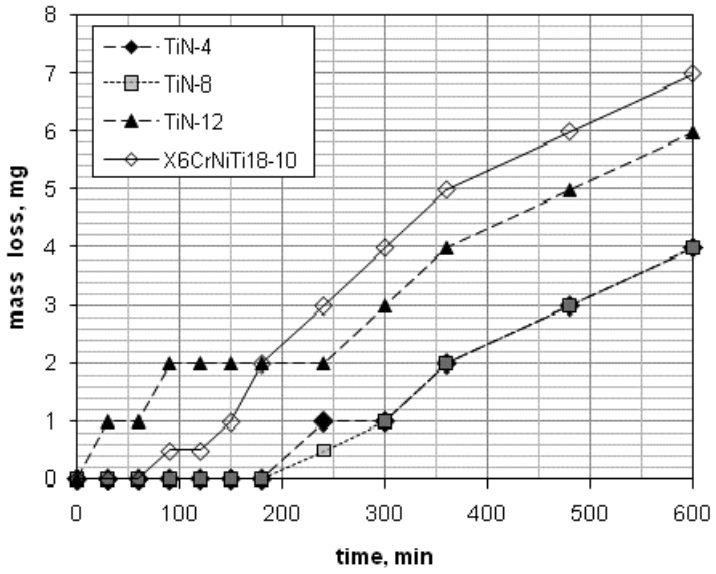

Fig. 5. Cavitation curves of specimens coated with various thickness of TiN coating

SEM observations have revealed the TiN coatings' damage (Fig. 6-8). The TiN-4 coating (Fig. 6) has deform plastically, cracks have arisen mostly on the top of micro-folds (Fig. 6 a). Cracks have developed by migrating through concave traces of post-microdroplets (Fig. 6 b). The microscope observations illustrate the initiation of microcracks appears at concave traces of post - Ti(N) microdroplets and on the boundary Ti(N) microdroplets and coating. Fig. 6 c suggests that delamination occurred at the side of micro-folds. At delamination areas microcracks arise in brittle mode especially when associated with coating defects (Fig. 6 c). At some spots (Fig. 6 d) the coating was pushed into the substrate. Probably it was caused by a collapsing cavitation

bubble in the vicinity of the surface; the marks have characteristic round shape. At intensive degraded areas the TiN coating was totally removed; there the erosion process continues into the substrate.

The cavitation erosion mechanism of TiN-8 (Fig. 7) coating is seen to differ essential in comparison to TiN-4 (Fig. 6). Although nearly all micro-droplets were removed (Fig. 7 a) there was no noticeable micro-folding. The coating was removed in the form of thin flakes. This suggests that the coating was degraded in layers. There were no sights that microcracks have occurred at the discontinuous spots (Fig. 7b), impacting water microjet have generated "cavitation tunnels" (Fig. 7c), which have penetrated into the coating. Coating was removed in brittle mode. On some places were visible typical feature of fatigue fracture for hard materials: cycling crack growth lines.

The TiN-12 coating was also removed in the form of thin flakes (Fig. 8); what is similar to degradation of TiN-8 coating (Fig.7). On the surface some micro-droplets were seen although the process of coating degradation had started (Fig. 8 a). This could mean that coating degradation process began in the very early stage of cavitation and the material was removed easier than Ti(N) micropdroplets. The coating was removed in layers in the form of flakes. Some cycling crack growth lines are visible on Fig. 8 b.

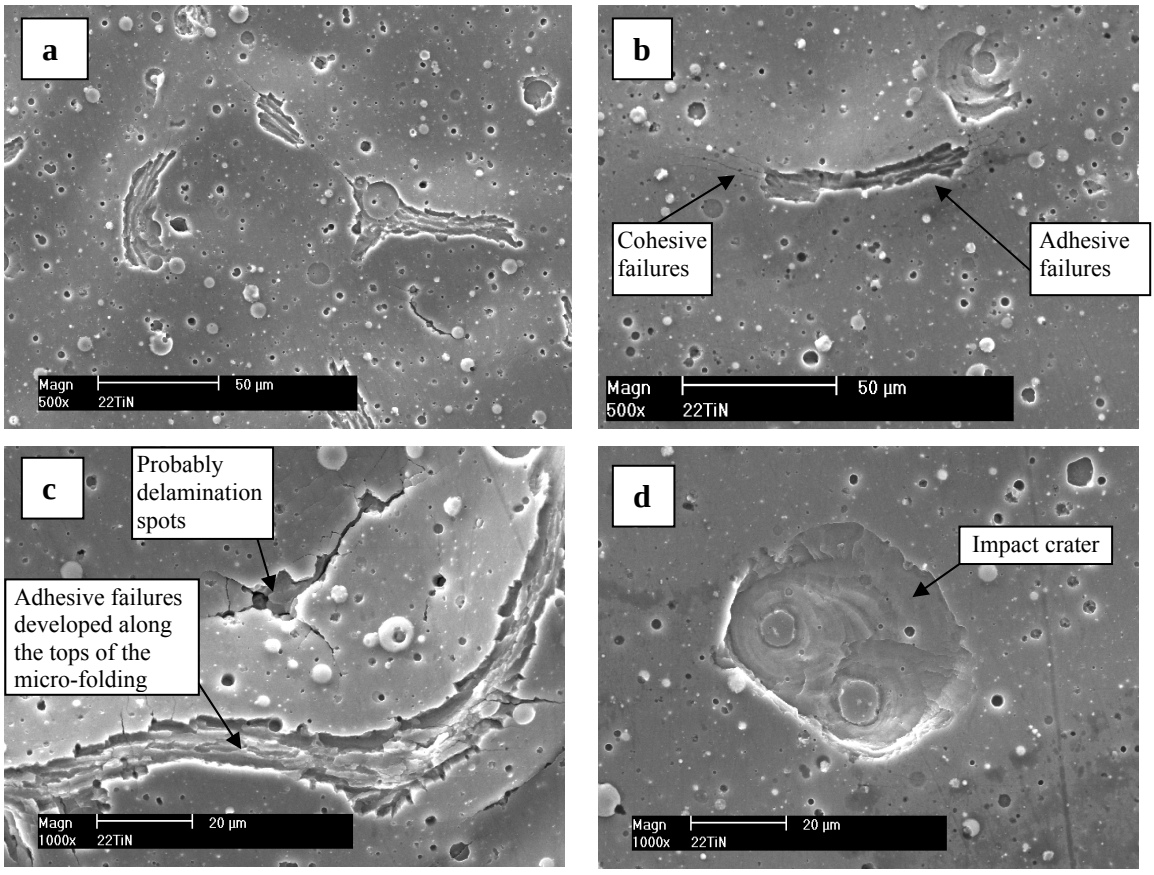

Fig. 6. SEM surface images of TiN-4 specimen after the cavitation test

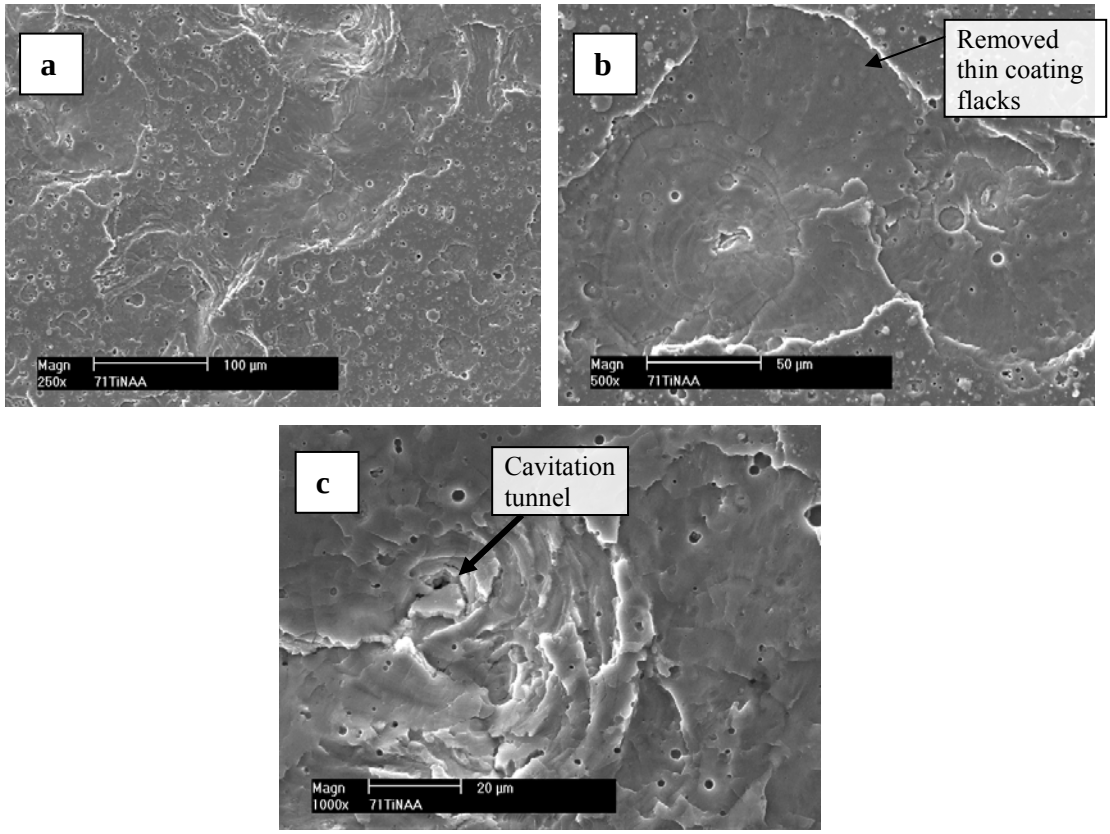

Fig. 7. SEM surface images of TiN-8 specimen after the cavitation test

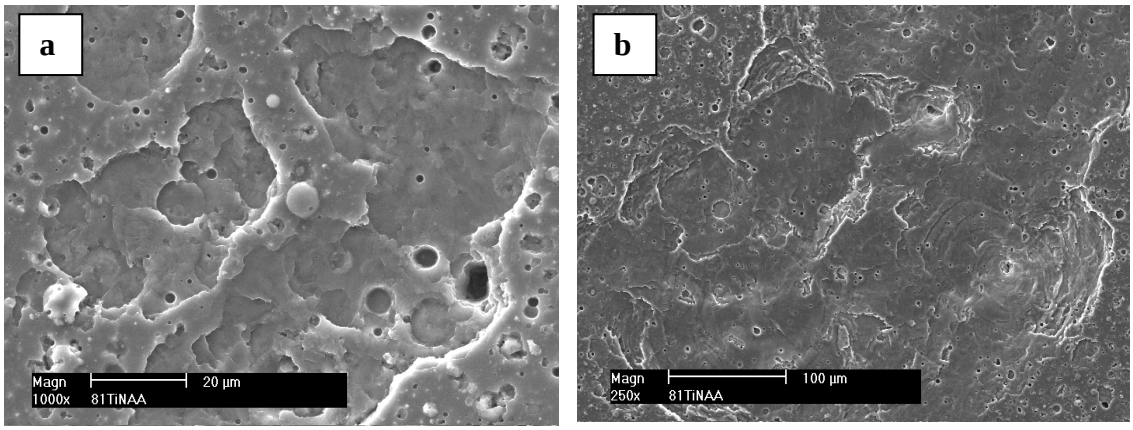

Fig. 8. SEM surface images of TiN-12 specimen after the cavitation test

DISCUSSION

An increase of coating thickness has caused an decrease of H/E parameter, the ratio of hardness (H) and elastic modulus (E), and coating critical load L_{C2} (Tab. 3). With the decrease of H/E ratio the impact-wear behaviour of the system changes from brittle to ductile mode. This means that with increase the H/E parameter the coating is more and more ductile. In the case of present investigation the TiN coatings (Tab. 3) exhibit H/E

parameters of 0.063, 0.060 and 0.058 for TiN-4, TiN-8, TiN-12 coatings, respectively. The cavitation test has revealed that the cavitation resistance of the TiN-4 coating is identical with the TiN-8 coating; both coatings had the same incubation period and the same mass loss after the whole cavitation test, despite the fact that the H/E parameter of the TiN-4 coating is higher than the TiN-8 coating's. The TiN-12 coating possesses the lowest H/E parameter and the highest mass loss. These investigations show that the decrease H/E parameter do not validate the improvement in cavitation wear of TiN coatings.

Microscopic observations of the TiN-4 coating (Fig. 6) have revealed that this coating underwent micro-folding. The micro-undulation of the TiN-4 coating evidence that this coating had ability to plastic deformation, although cracks shown in Fig. 6 had brittle character. Ma et al [12] have found that plastic deformation of TiN coating occurred via cracking and sliding along the inter-columnar grain boundaries at contact surface with the substrate, where the highest tension stresses are. The first micro-cracks were observed on the top of micro-folds (Fig. 6). This could evidence that the highest tension stresses are at the top of micro-folds. The microcracks were probably initiated due to arising tensile stresses that exceed the coating toughness. Additionally existing discontinuously areas, i.e. concave traces of post-microdroplets where the cross-section was lesser, were conducive to initiating microcracks. Micro-cracks expanded farther through concave traces of post-microdroplets (Fig. 6b). It shows that coating defects affect the acceleration of the microcracks growth. Cyclic loading caused by repeated action of cavitation bubbles has been found to cause substrate deformation, which likely occurs faster than the deformation of the coating [11, 12]. This could lead to coating delamination. Delamination spots occurred at the side of the micro-folds (Fig. 6c).

Microscopic observations of the TiN-8 coating (Fig. 7) have shown the change in degradation mechanism in relation to the TiN-4 coating (Fig. 6). The TiN-8 coating was removed in the form of flakes in a brittle manner and no plastic deformation (micro-undulation) was visible. Similar degradation mechanism is seen on the TiN-12 specimen.

On all TiN coatings occur impurities (visible on Fig. 3), which are Ti(N) micro-droplets. With increase coating thickness the number of micro-droplets increased as well. Moreover, the fracture images (Fig. 3) shows that inside the coatings with thickness of 7.8 and 11.9 μm some discontinuity spots in coating structure occurred in the form of cavities. Münsterer and Kohlhof [13] noticed that all discontinuity spots in coating act as nucleation centres for wear. If we assume that the number of cavities inside coating is proportional to the number of micro-droplets on the coating surface, then the coating endurance lessens essential with the coating thickness. This might be the reason for very low cavitation resistance of TiN-12 coating.

In many analyses the implosion of cavitation bubbles in the surrounding of the solid was compared to the impact of a ball. Such comparison was made e.g. by Bogachev [4]. In such situation we can consider cavitation erosion as special case of bubble impact loading wear and treat cavitation degradation as a contact fatigue. Therefore we can use some aspects of Hertz theory to our analysis. In the case of contact stresses analysis, there is place under the surface at which the highest shear stress occurred. This place is co-called "Bielajew's point". This point depends on the diameter of a ball, the impact force and Young modulus. The major problem is to assess the diameter of a cavitation bubble. The diameter of a cavitation bubble is in the range from μm to mm. Numachi [21] obtained in his study that the diameter of a cavitation bubble is approximately 117 μm, whereas Ivany and Hammit [22] in their calculations assume that the reference

initial bubble radius is 1.27 mm. The sensitive issue in the diameter assessment is the change of the bubble diameter during bubble implosion. This explains essential difference in bubbles diameter between researchers. To estimation I take into consideration the bubble radius suggested by Hammit [3]. Next problem is the amplitude of the pressure pulse in a given cavitation condition; it is known that cavitation pulses can vary in wide range depending on cavitation conditions.

The assessment of the impact force of cavitation bubble is very difficult due to wide range of pressure amplitude [24]. Previously performed measurements using 113A72 PCB Piezotronics pressure transducers of 0 - 35 MPa measurement range, 0.148 mV/kPa sensitivity, 450 kHz resonance frequency and 4.5 mm effective membrane diameter [23] showed that the pressure amplitude of 3.5 MPa seems to be quite reasonable because of number of pulses in 1s. Pulses with lower amplitude were much more, but the amplitude seems to be too low to cause any damage in material.

Taking into account all mentioned above data we obtained that the Bielajew's point is positioned 4.0, 3.7 and 3.5 μm under the surface, respectively for TiN-4, TiN-8 and TiN-12. The shear stress at this point varies from approx. 990 MPa to 1300 MPa depending on coating thickness (Young's modulus of the TiN coatings). The thicker the coating, the Bielajev point is closer the surface and the shear stresses are higher. We should mention that those calculations are only roughly calculations. Nevertheless, presented calculations show the possibility of micro-crack initiation below and parallel to the surface. Moreover, they show that the process of the fretting is possible for coatings with thickness higher than 4 μm and the delamination process might occur for coatings with thickness of 3.9 μm.

SUMMARY AND CONCLUSIONS

The study presents assessment of cavitation resistance of TiN coatings with three different thicknesses deposited on austenitic X6CrNiTi18-10 steel by cathodic arc evaporation method. It was affirmed that the cavitation resistance is related with adhesion of the TiN coating and coating thickness.

The obtained results and their analysis allow the following conclusion:

- The increase of coating thickness of TiN coatings had an influence on coating's mechanical properties (increase of coating stiffness and adhesion). The same good cavitation resistance was obtained for the TiN-4 and the TiN-8 coatings.
- The increase of coating thickness has caused the increase the number of coating defects.
- All discontinuous spots reduce coating durability and enhance cavitation erosion.
- The increase of coating thickness has caused the change of coating degradation mechanism.
- The cavitation resistance of the TiN-4 coating was similar to the TiN-8 coating, whiles the increase of the TiN coating thickness to 12 μm caused the decrease of the TiN coating's cavitation resistance.

ACKNOWLEDGEMENTS

The author wishes to thank warmly dr Andrzej Czyżniewski, Koszalin University of Technology, Institute of Mechatronics, Nanotechnology and Vacuum Technique, for the deposition of TiN coatings, and for performing the adhesion measurements.

REFERENCES

1. Bourne N.K.: On the collapse of cavities. Shock Waves 11 (2002), pp. 447-455.
2. Philipp A., Lauterborn W.: Cavitation erosion by single laser-produced bubbles. J.Fluid Mech. 361 (1998), pp.75-116.
3. Hammit F.G.: Cavitation and multiphase flow phenomena. McGraw-Hill Inc. 1980.
4. Heymann F. J.: On the time dependence of the rate of erosion due to impingement or cavitation. ASTM 408, Baltimore 1967, pp. 70-100.
5. Bogachev I.N., Mints R.I.: Cavitational erosion and means for its prevention. Israel program for Scientific Translations Ltd., Jerusalem 1966.
6. Heathcock C.J., Protheroe B.E., Ball A.: Cavitation erosion of stainless steels. Wear 81 (1982), pp.311-327.
7. Thiruvengadam A.: A unified theory of cavitation damage, Transactions of the ASME, Journal of Basic Engineering 85 (1963), pp.365-376.
8. Iwai Y., Honda T., Yamaa H., Matsumura T., Larsson M., Hogmark S.: Evaluation of wear resistance of thin hard coatings by a new solid particle impact test. Wear (2001),pp. 861-867.
9. Yoon S.Y., Yoon S.Y., Chung W.S., Kim K.H.: Impact-wear behaviors of TiN and Ti-Al-N coatings na AISI D2 steel and WC-Co substrates. Surface and Coating Technology 177-178 (2004), pp.645-650.
10. Voevodin A.A., Bantle R., Matthews A.: Dynamic impact wear of TiC_xN_y and Ti-DLC composite coatings. Wear 185 (1995), pp.151-157.
11. Cairney J.M., Tsukano R., Hoffman M.J., Yang M.: Degradation of TiN coating under cyclic loading. Acta Materialia 52 (2004), pp. 3229-3237.
12. Ma L.W., Cairney J.M., Hoffman M., Munroe P.R.: Deformation mechanisms operating nanoindentation of TiN coatings on steel substrates. Surface & Coatings Technology 192 (2005), pp.11-18.
13. Münsterer S., Kohlhof K.: Cavitation protection by low temperature TiCN coatings. Surface and Coatings Technology 74-75 (1995), pp. 642-647.
14. Marynin V.H.: Erosion of vacuum-arc Ti-N coatings. Materials Science 39 (2003), pp. 447-451.

15. Krella A., Czyżniewski A.: Influence of the substrate hardness on cavitation erosion resistance of TiN coating. Wear 263 (2007), pp. 395-401.
16. Krella A., Czyżniewski A.: Investigation concerning the cavitation resistance of TiN coatings deposited on austenitic stainless steel at various temperatures. Wear 265 (2008), pp. 72-80.
17. Leyland A., Matthews A.: On the significance of the H/E ratio in wear control: a nanocomposite coating approach to optimized tribological behaviour. Wear 246 (2000), pp. 1-11.
18. Lima M.M., Godoy C., Modenesi P.J., Avelar-Batista J.C., Davoson A., Matthews A.: Coating fracture toughness determined by Vickers indentation: an important parameter in cavitation erosion resistance of WC-Co thermally sprayed coatings. Surface and Coating Technology 177-178 (2004), pp. 489-496.
19. Han S., Lin J.H., Kuo J.J., He J.L., Shih H.C.: The cavitation-erosion phenomenon of chromium nitride coatings deposited using cathodic arc plasma deposition on steel. Surface and Coating Technology 161 (2002), pp. 20-25.
20. Oliver W.C., Pharr G.M.: An improved technique for determining hardness and elastic modulus using load and displacement sensing indentation experiments. J Mater Res 7 (1992), pp. 1564-1583.
21. Numachi F.: An experimental study of accelerated cavitation induced by ultrasonics. J. Basic Engineering 87 (1965), pp. 967-976.
22. Ivany R.D., Hammit F.G.: Cavitation bubble collapse in viscous, compressible liquids – numerical analysis. J. Basic Engineering 87 (1965), pp. 977-984.
23. Steller J., Krella A., Koronowicz J., Janicki J.: Towards quantitative assessment of material resistance to cavitation erosion. Wear 258 (2005), pp. 604-613.